

## Polypyrrole/MnO<sub>2</sub> Composites and Their Enhanced Electrochemical Capacitance

Ai-Qin Zhang, Yuan-Hua Xiao, Ling-Zhen Lu, Li-Zhen Wang, Feng Li

Henan Provincial Key Laboratory of Surface and Interface Science, Zhengzhou University of Light Industry, Zhengzhou 450002, China

Correspondence to: F. Li (E-mail: lifeng696@yahoo.com)

**ABSTRACT:** The composites of polypyrrole (PPY) and MnO<sub>2</sub> have been prepared through chemical oxidation of pyrrole monomer and MnO<sub>2</sub> suspension with ammonium peroxydisulfate at low temperature. The morphology and structure of materials were characterized by Fourier transform infrared spectroscopy (FTIR), scanning electron microscope (SEM), Transmission electron microscopy (TEM), thermal gravity analysis - differential thermal gravity (TG-DTG), and X-ray diffraction (XRD) measurements. The electrochemical properties of the composite were investigated by galvanostatic charge-discharge and electrochemical impedance spectroscopy. The specific capacitance of the composite electrode is 352.8 F/g at a current of 8 mA/cm<sup>2</sup> in Na<sub>2</sub>SO<sub>4</sub> electrolyte of 0.5 mol/L, which is much higher than that of 246.2 F/g and 103.5 F/g of PPY and MnO<sub>2</sub>, respectively. A convenient and effective technique has been developed to fabricate composite materials of PPY and MnO<sub>2</sub> promising for designing new capacitors. © 2012 Wiley Periodicals, Inc. *J. Appl. Polym. Sci.* 000: 000–000, 2012

**KEYWORDS:** polypyrrole; MnO<sub>2</sub>; composite; electrochemical capacitance; electrochemistry

Received 1 May 2012; accepted 3 June 2012; published online

DOI: 10.1002/app.38153

### INTRODUCTION

Electrochemical capacitors (ECs) or supercapacitors have attracted considerable attention as a novel energy-storage device with high power density and long cycling durability. As the performance of ECs depends primarily on the electrochemical performance of electrode material,<sup>1,2</sup> more and more researchers focused on finding suitable substance used as electrode materials. Carbon,<sup>3,4</sup> transition metal oxides,<sup>5,6</sup> and conducting polymers<sup>7–9</sup> are widely applicable materials, of which metal oxides and conducting polymers represent promising material for the application of supercapacitors due to their high Faraday pseudocapacitance.

At the same time, as electrode material for supercapacitor, transition metal oxides, and electrically conducting polymers (ECPs) have some problems that limit their further application and industrialization. For example, transition metal oxides such as hydrous RuO<sub>2</sub>, NiO, CoOx, and MnO<sub>2</sub> have been studied and implemented as electrode materials for ECs. Although they have wide charge-discharge potential range, most of the transition metal oxides have relatively low specific capacity.<sup>10–15</sup> Comparatively, conducting polymers such as polyaniline and polypyrrole (PPY) show high specific capacitance, but the relatively low mechanical stability and cycle life are major limitations for applications.<sup>16–19</sup> There are also some literatures about the composites of

PPY and manganese dioxide,<sup>20–23</sup> which show better electrochemical capacitive performance than single component. These composites usually need intricate synthesis conditions, so it is difficult to industrialization for them to be used as electrode material of ECs.

In this article, the composite of PPY and electrolytic manganese dioxide (EMD) was prepared by one-pot chemical synthesis. By this method, we want to find an economic and effective way to get a widely applicable material. Additionally, more important aim was to obtain a new electrode material with good electrochemical performance. So, its capacitive behavior was examined by cyclic voltammetry, galvanostatic charge-discharge, and electrochemical impedance spectroscopy (EIS).

### EXPERIMENTS

#### Synthesis of PPY/MnO<sub>2</sub> Composites

Pyrrole (Py, 99%, Fluka, Switzerland) were purified through distillation under reduced pressure and stored refrigerated before use. MnO<sub>2</sub> used in this work was EMD (Xiangtan Electrochemical Scientific), and all other reagents were analytically pure and used directly without purification.

The synthesis of PPY/MnO<sub>2</sub> was carried out at constant temperature of 0°C. First, FeCl<sub>3</sub> (oxidant) was dissolved in 1 mol/L hydrochloric acid, stirring and putting EMD into the mixtures.

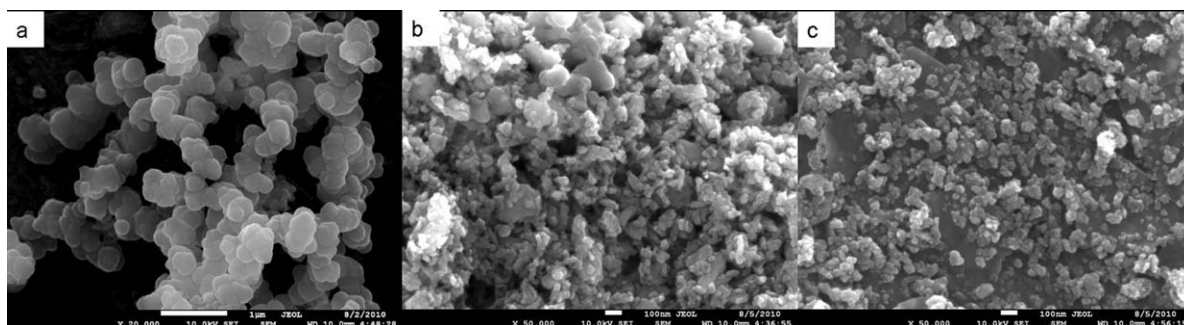


**Figure 1.** SEM images of polypyrrole (a), MnO<sub>2</sub> (b), and polypyrrole/MnO<sub>2</sub> (c) composites.

Second, after 1 h of stirring, Py was added into the above solution. The molar ratio of Py to MnO<sub>2</sub> was 1 : 3. Lastly, the precipitates were separated by filtration, rinsed with 0.01 mol/L HCl, water, and acetone for three times, respectively, and dried at 60°C in a vacuum oven to yield black powders. In comparison, PPY materials were synthesized at the same experimental parameters.

#### Structure Characterization

The materials were analyzed by scanning electron microscope (FESEM, JSM-7001F), Transmission electron microscopy (HRTEM, TEM-2100) Fourier transform infrared spectroscopy (FTIR, BRUKER-EQUINOX-55), Pyris Diamond (Diamond TG/DTA), and X-ray diffraction (XRD, PW-3710).

#### Preparation of Electrodes

The composites for fabricating electrode were prepared by mixing active materials (80 wt %), carbon blacks (10 wt %), and polytetrafluoroethylene (10 wt %) and stirring at 25°C for 1 h to mixed thoroughly. The materials were then coated on the surface of nickel foam (1 cm<sup>2</sup>), dried at 60°C for 8 h, and pressed at 15 MPa to get PPY/MnO<sub>2</sub> electrode. Electrodes of PPY and EMD were also prepared with the same procedure described above.

#### Electrochemical Tests

All electrochemical tests were carried out in a three-electrode cell configuration with a platinum counter electrode and a standard calomel reference electrode (SCE). The electrolyte was 0.5 mol/L Na<sub>2</sub>SO<sub>4</sub>.

The electrochemical behaviors of the composite electrode were evaluated by galvanostatic charge–discharge and EIS techniques

with electrochemical workstation (CHI660D) at room temperature. The galvanostatic charge–discharge test was carried at different current density with potential window range of 0.005–1 V (vs. SCE). EIS measurement was performed at open-circuit potential with frequency in the range of 5 mHz – 100 kHz.

## RESULTS AND DISCUSSION

### Characterization of the PPY/MnO<sub>2</sub> Composites

SEM and TEM images of PPY, MnO<sub>2</sub>, and PPY/MnO<sub>2</sub> composites are shown in Figures 1 and 2. It can be seen that pure PPY is granular and about 200–300 nm in diameter, whereas the image of MnO<sub>2</sub> shows tiny and uneven particles. When compared with PPY and MnO<sub>2</sub>, the pellets of composites are smaller and more even, about 30–50 nm in diameter, which is favorable for fabricating electrode material of supercapacitors because the composite electrode would show high double-layer capacitance as well as pseudocapacitance.

The FTIR spectra of PPY and the PPY/MnO<sub>2</sub> composite are presented in Figure 3. It can be seen that all the main characteristic peaks of PPY can be found both at the infrared spectrum of the composites and that of PPY. For example, the main characteristic peaks of PPY are assigned as follows: the bands at 1564 cm<sup>-1</sup>, 1480 cm<sup>-1</sup> correspond to C=C and C–C stretching, and the bands at 1298 cm<sup>-1</sup>, 1240 cm<sup>-1</sup> belong to C–N stretching mode. The C–C breathing and C–H out of plane vibration are at 1122 cm<sup>-1</sup> and 798 cm<sup>-1</sup>, respectively. The corresponding peaks in the spectrum of the composites are at 1547 cm<sup>-1</sup>, 1464 cm<sup>-1</sup>, 1310 cm<sup>-1</sup>, 1187 cm<sup>-1</sup>, 1045 cm<sup>-1</sup>, and 910 cm<sup>-1</sup>.

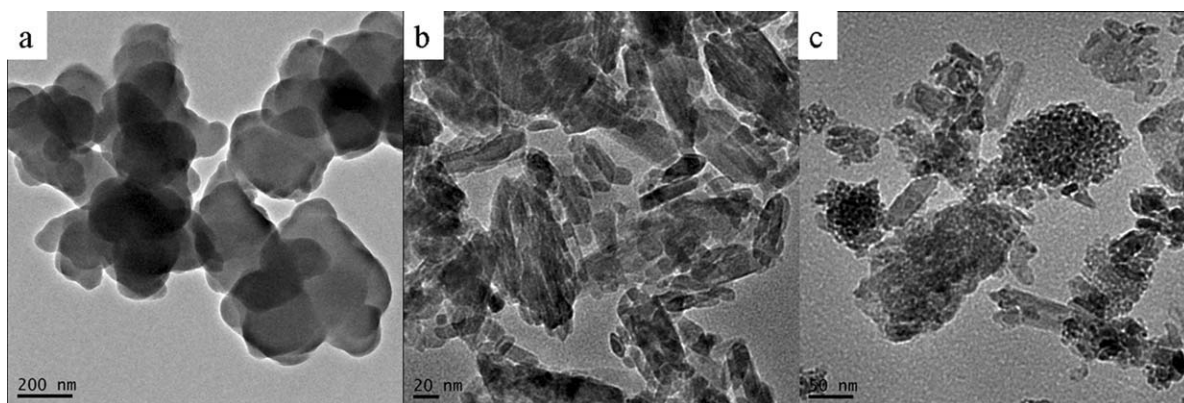


**Figure 2.** TEM images of polypyrrole (a), MnO<sub>2</sub> (b), and polypyrrole/MnO<sub>2</sub> (c) composites.

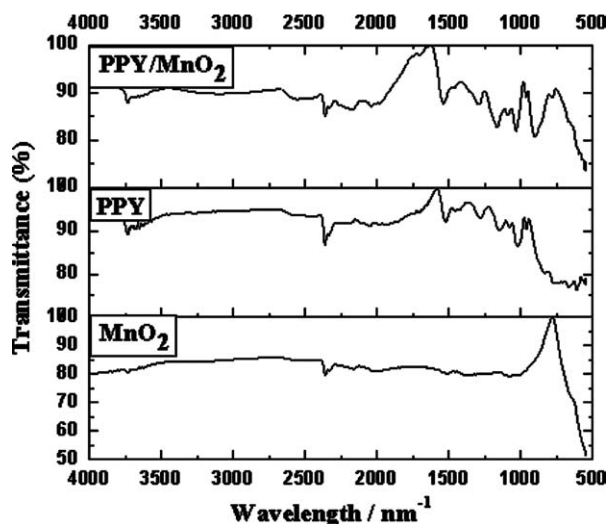


Figure 3. FTIR spectra of PPY and polypyrrole/MnO<sub>2</sub> composites.

When compared with the peaks of PPY, red shift occurs at the infrared spectrum of the composites, which maybe attribute to the charge transfer after the MnO<sub>2</sub> combined to the PPY chains. The above results indicate that the PPY/MnO<sub>2</sub> composites were indeed obtained in the process of one-pot chemical synthesis.

In addition, PPY, MnO<sub>2</sub>, and MnO<sub>2</sub>/PPY composites were also confirmed by the XRD patterns as given in Figure 4. As appeared in the XRD graph, pure PPY indicates a broad peak between 20 and 30 of 2θ value, which indicates that the PPY is in amorphous form. Although the MnO<sub>2</sub> particles are mixed by β-MnO<sub>2</sub> with little α-MnO<sub>2</sub> from the XRD pattern. From the XRD pattern of the composites, some diffraction peaks of MnO<sub>2</sub> can be seen with lower intensity compared with pure EMD.

Figure 5 shows the TG-DTG curves of the MnO<sub>2</sub>/PPY composites. It can be seen that there are three weight loss processes from 0 to 800°C, of which weight loss blow 100°C was the evaporation of residue water in the sample. From 100°C to 630°C,

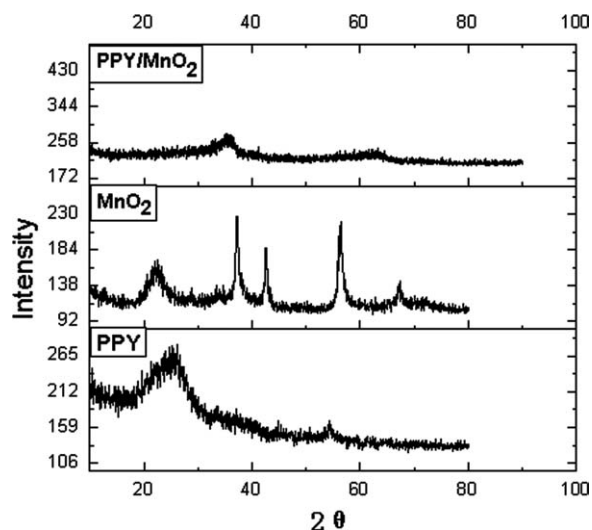


Figure 4. XRD patterns of PPY, MnO<sub>2</sub>, and MnO<sub>2</sub>/PPY composites.

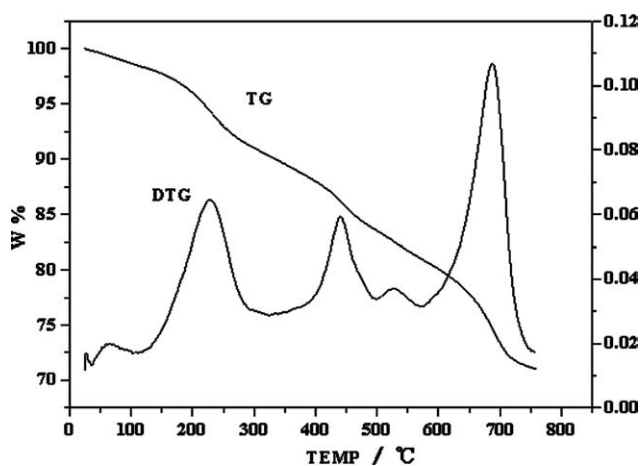


Figure 5. TG-DTG curves of the MnO<sub>2</sub>/PPY composites.

the weight loss (about 20%) maybe due to decompose of PPY and some impurity components of the composites. Pyrogenic decomposition of PPY mainly occurred at 630–700°C, and at 655°C the decomposition rate is the highest. After heated to 800°C, the sample residues are about 49.57%, which could prove that the composites are composed of PPY and MnO<sub>2</sub>.

#### Electrochemical Capacitance of the PPY/MnO<sub>2</sub> Composites

Figure 6 shows the galvanostatic charge–discharge curves of PPY, MnO<sub>2</sub>, and the composite electrode at a constant current of 8 mA/cm<sup>2</sup>. The discharge time increased in the order of MnO<sub>2</sub> < PPY < PPY/MnO<sub>2</sub> composites, and it can be calculated based on Figure 4 that the specific capacitance of these electrodes are 103.5 F/g, 246.2 F/g, and 352.8 F/g, respectively. It is obvious that the composite electrodes show much higher specific capacitance and are promise candidates for designing supercapacitors.

The specific capacitance of the composite electrode decreased with cycle number, as showed in Figure 7. After cycled 100

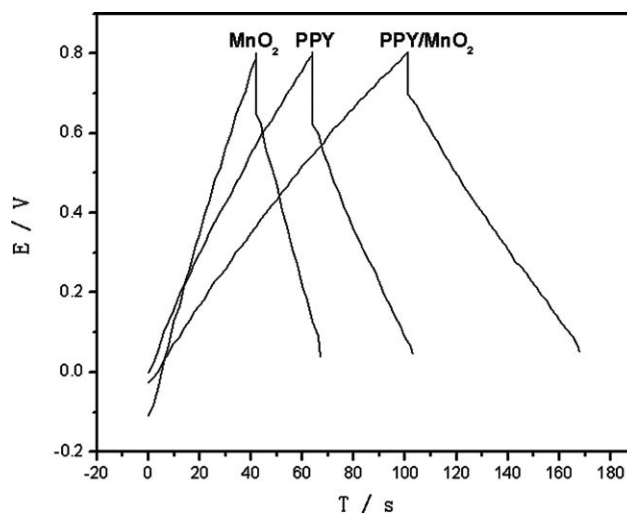
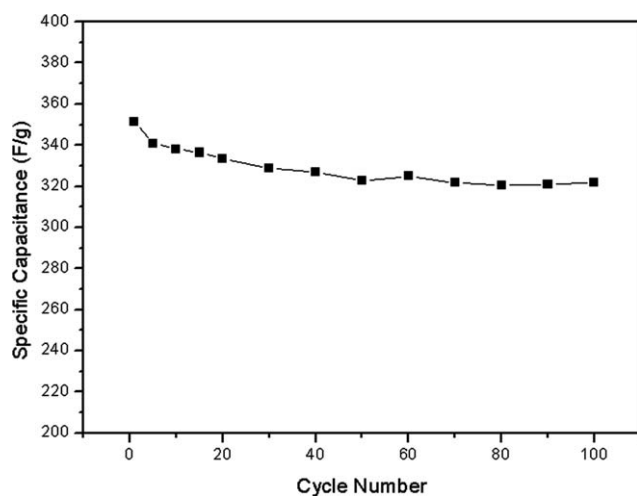


Figure 6. Galvanostatic charge–discharge curves of PPY, MnO<sub>2</sub>, and PPY/MnO<sub>2</sub> composite electrode at a current density of 8 mA/cm<sup>2</sup>.



**Figure 7.** Variation of discharge specific capacity with cycle number of a PPY/MnO<sub>2</sub> composite electrode.

times, the specific capacitance changed to 321.7 F/g, about 91.2% of the initial value. In the process of charge–discharge, some of the active material may decompose with cycling and capacity deattenuation occurred subsequently. The value after cycled 100 times is also accepted for electrode material of supercapacitors.

For comparison, we chosen different molar ratio of Py and MnO<sub>2</sub> to prepare the composites. The specific capacities of these composites before and after 100 cycles were listed in Table I. If the molar ratio of Py to MnO<sub>2</sub> was too high, for example 1 : 1 or 1 : 2, the composite showed low mechanical stability and poor cycling performance. If the proportion of MnO<sub>2</sub> was too high, the specific capacity was low. We chose 1 : 3 as molar ratio of Py to MnO<sub>2</sub> for synthesis of PPY/MnO<sub>2</sub> composites.

The impedance responses of PPY, MnO<sub>2</sub>, and PPY/MnO<sub>2</sub> composite electrode are displayed in Figure 8, which was carried out at the open circuit potential in the frequency range of 0.005–105 Hz with ac-voltage amplitude of 10 mV. For MnO<sub>2</sub> and PPY electrode, the Nyquist plots consist of two parts: a single semi-circle in the high and medium frequency region and a straight line in the low-frequency region. Although for PPY/MnO<sub>2</sub> composite electrode, the impedance responses in the high and medium frequency region are different from other two. Because the information from high and medium frequency regions can be attributed to the double layer charging process

**Table I.** The Specific Capacities of the Composites Prepared with Different Molar Ratio (Pyrrole to MnO<sub>2</sub>) before and after 100 Cycles

	1 : 1	1 : 2	1 : 3	1 : 4	1 : 5
First specific capacity (F/g)	318.4	349.8	352.8	196.3	121.8
Specific capacity after 100 cycles (F/g)	238.8	286.8	321.7	188.4	117.5

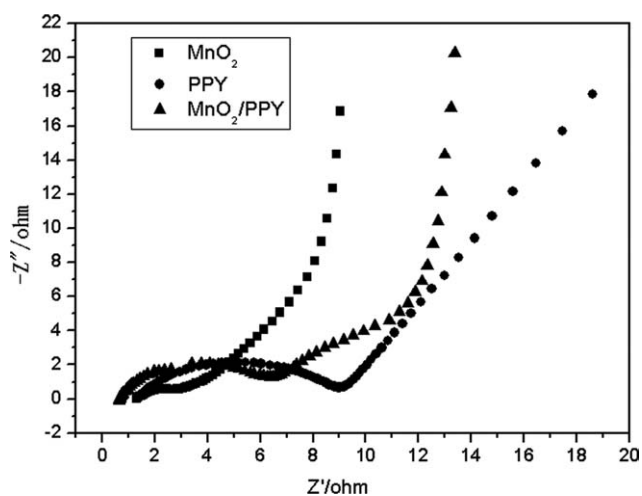


**Figure 8.** Nyquist diagram of PPY, MnO<sub>2</sub>, and PPY/MnO<sub>2</sub> composite electrode in 0.5 mol/L Na<sub>2</sub>SO<sub>4</sub> at open circuit potential.

and also to the charge transfer step, the difference in the Nyquist plots can explain why the composite electrode shows better electrochemical performance and high specific capacitance.

## CONCLUSIONS

A suitable capacitive material for supercapacitors, PPY/MnO<sub>2</sub> composites have been prepared by one-pot chemical synthesis. The electrochemical capacitive performance of the composite had been evaluated by galvanostatic charge–discharge and EIS. The results indicate that PPY/MnO<sub>2</sub> composites have better capacitive performance than PPY and MnO<sub>2</sub>, and the specific capacitance of the composite electrode was 352.8 F/g in 0.5 mol/L Na<sub>2</sub>SO<sub>4</sub> at a current density of 8 mA/cm<sup>2</sup>. These promising results, combined with the convenient and effective technique, make this composite an exceptional choice for electrode material of ECs.

## ACKNOWLEDGMENTS

This work was supported by National Science Foundation of China (NSFC) under grant 21071130 and the Outstanding Scholar Foundation of Henan Province.

## REFERENCES

- Zhang, Y.; Feng, H.; Wu, X. B.; Wang, L. Z.; Zhang, A. Q.; Xia, T. C.; Dong, H. C.; Li, X. F.; Zhang, L. S. *Int. J. Hydrogen Energy* **2009**, *34*, 4889.
- Burke, A. *Electrochim. Acta* **2007**, *53*, 1083.
- Ania, C. O.; Pernak, J.; Stefaniak, F.; Raymundo-Piñero, E.; Béguin, F. *Carbon* **2009**, *47*, 3158.
- Xia, N. N.; Zhou, T. X.; Mo, S. S.; Zhou, S. L.; Zou, W. J. *J. Appl. Electrochem.* **2011**, *41*, 71.
- Wen, J. G.; Ruan, X. R.; Zhou, Z. T. *J. Phys. Chem. Solids* **2009**, *70*, 816.
- Kuratani, K.; Tanaka, H.; Takeuchi, T.; Takeichi, N.; Kiyobayashi, T.; Kuriyama, N. *J. Power Sources* **2009**, *191*, 684.



7. Zhao, G. Y.; Li, H. L. *Microporous Mesoporous Mater.* **2008**, *110*, 590.
8. Ribeiro, L. M. O.; Auad, J. Z.; Silva, J. G., Jr.; Navarro, M.; Mirapalheta, A.; Fonseca, C.; Neves, S.; Tonholo, J.; Ribeiro, A. S. *J. Power Sources* **2008**, *177*, 669.
9. Frackowiak, E.; Khomenko, V.; Jurewicz, K.; Lota, K.; Béguin, F. *J. Power Sources* **2006**, *153*, 413.
10. Liang, Y. Y.; Li, H. L.; Zhang, X. G. *J. Power Sources* **2007**, *173*, 599.
11. Xing, W.; Li, F.; Yan, Z. F.; Lu, G. Q. *J. Power Sources* **2004**, *134*, 324.
12. Yu, Y.; Ji, G. b.; Cao, J. M.; Liu, J. S.; Zheng, M. B. *J. Alloys Compd.* **2009**, *471*, 268.
13. Li, J. L.; Gao, F.; Jing, Y.; Miao, R. Y.; Wu, K. Z.; Wang, X. D. *Int. J. Miner. Process.* **2009**, *16*, 576.
14. Adelkhani, H.; Ghaemi, M. *J. Alloys Compd.* **2010**, *493*, 175.
15. Kuratani, K.; Kiyobayashi, T.; Kuriyama, N. *J. Power Sources* **2009**, *189*, 1284.
16. Kim, B. C.; Kwon, J. S.; Ko, J. M.; Park, J. H.; Too, C. O.; Wallace, G. G. *Synth. Met.* **2010**, *160*, 94.
17. Shi, L.; Wu, X. D.; Lu, L. D.; Yang, X. J.; Wang, X. *Synth. Met.* **2010**, *160*, 989.
18. Huang, S. C.; Huang, S. M.; Ng, H.; Kaner, R. B. *Synth. Met.* **1993**, *57*, 4047.
19. Kurzweil, P. *Encyclopedia Electrochem. Power Sources* **2009**, *24*, 679.
20. Li, J.; Cui, L.; Zhang, X. *Appl. Surf. Sci.* **2010**, *256*, 4339.
21. Hashmi, S. A.; Upadhyaya, H. M. *Ionics* **2002**, *8*, 272.
22. Sivakkumar, S. R.; Ko, J. M.; Kim, D. Y.; Kim, B. C.; Wallace, G. G. *Electrochim. Acta* **2007**, *52*, 7377.
23. Sharma, R. K.; Rastogi, A. C.; Desu, S. B. *Electrochim. Acta* **2008**, *53*, 7690.